Photoemission Properties of Methyl-Substituted Guanines: Photoelectron and Fluorescence Investigations of 1,9-Dimethylguanine, O^6,9-Dimethylguanine, and 9-Methylguanine

Pierre R. LeBreton,*,† Xu Yang,† Shigeyuki Urano,† Sharon Fetzer,† Min Yu,† Nelson J. Leonard,*,‡ and Shiv Kumar‡

Contribution from the Department of Chemistry, University of Illinois at Chicago, Chicago, Illinois 60680, and Department of Chemistry, University of Illinois at Urbana—Champaign, Urbana, Illinois 61801. *Received June 5, 1989*

Abstract: Photoelectron and fluorescence emission properties of 1,9-dimethylguanine (1,9-DMG), O^6,9-dimethylguanine (O^6,9-DMG), and 9-methylguanine (9-MG) have been examined. Gas-phase HeI photoelectron spectra have been compared with theoretical ionization potentials provided by HAM/3 semiempirical quantum mechanical calculations, and by SCF ab initio calculations carried out with 3-21G and 4-31G basis sets. Geometries of 1,9-DMG and O^6,9-DMG used in the calculations were based on X-ray crystallographic data measured in this investigation. For 1,9-DMG, which occurs in the amino keto form of guanine that participates in Watson–Crick base pairing, and for O^6,9-DMG, which is a model compound for mutagenic and carcinogenic products formed in DNA alkylation reactions, ionization potentials have been measured for 8 and 10 of the highest occupied orbitals, respectively. For 9-MG, which can occur in either an amino keto or an amino enol form, the present results suggest that both tautomers occur in the gas phase, but that the amino enol tautomer predominates. Measurements of fluorescence emission spectra indicate that protonated O^6,9-DMG has a higher fluorescence quantum yield than protonated 1,9-DMG or 9-MG. At a pH of 2.0 and at an excitation wavelength of 270 nm the relative emission intensities of O^6,9-DMG, 1,9-DMG, and 9-MG are 11.0, 1.0, and 1.2 respectively, and the fluorescence lifetimes are 5.4, 0.4, and 0.4 ns. Results from HAM/3 and CNDO/S CI calculations on N7-protonated O^6,9-DMG, 1,9-DMG, and 9-MG are consistent with the conclusion that the low fluorescence intensities of 1,9-DMG and 9-MG are related to the vibronic coupling of low-lying singlet $n\pi^*$ and $\pi\pi^*$ states, and to the occurrence of efficient intersystem crossing.

Electron and photon emission spectroscopies have enjoyed success as tools for probing the structure of nucleotides and for elucidating nucleotide chemical and biochemical interactions. Gas-phase UV photoelectron spectroscopy has provided an opportunity to experimentally test and scale theoretical molecular orbital descriptions of valence electrons in DNA and RNA components. This method has already been applied to all of the most common bases occurring in DNA and RNA,[1] to synthetic bases that act as antimetabolites,[2] to nucleosides,[3] to phosphate esters,[4] and to nucleotides.[5]

Fluorescence spectroscopy provides a highly sensitive method for detailing the structure of nucleotides and the interaction of nucleotides with aromatic ligands and proteins.[6] In previous studies at ambient temperature, the low quantum yields of DNA and RNA bases have often been exploited to simplify studies of systems containing nucleotides and molecules with high fluorescence emission intensities.[6] Interest has also focused on modified nucleotide bases with high fluorescence quantum yields. These include N^2,3-ethenoguanine and 1,N^6-ethenoadenine and its riboside and ribotides.[7] At low pH O-alkylated purines and pyrimidines also exhibit high fluorescence intensities.[8,9] An important feature of O-methylated and -ethylated nucleotide bases is that these molecules are formed in both in vivo and in vitro DNA alkylation reactions with mutagens and carcinogens such as nitrosoureas, nitrosamines, dialkylsulfates, and alkyl alkanesulfonates.[9-12] The resistance of O-alkylated purines in polynucleotides to depurination reactions,[10] and the generally refractive properties of O-alkylated bases toward DNA repair,[11] point to the potential significance of these products in mutagenic and carcinogenic mechanisms.

Among the nucleotide bases, guanine poses some unique properties, which make a detailed understanding of its photoemission characteristics both difficult and interesting. With 78 electrons, guanine has the most complex electronic structure of all the nucleotide bases. Furthermore, recent IR studies in inert matrices suggest that guanine exhibits a greater tautomeric flexibility than that occurring among the other common nucleotide

† University of Illinois at Chicago.
‡ University of Illinois at Urbana—Champaign.

(1) (a) Padva, A.; LeBreton, P. R.; Dinerstein, R. J.; Ridyard, J. N. A. *Biochem. Biophys. Res. Commun.* **1974**, *60*, 1262. (b) Lauer, G.; Shäfer, W.; Schweig, A. *Tetrahedron Lett.* **1975**, *17*, 3939. (c) Hush, N. S.; Cheung, A. S. *Chem. Phys. Lett.* **1975**, *34*, 11. (d) Padva, A.; O'Donnell, T. J.; LeBreton, P. R. *Chem. Phys. Lett.* **1976**, *41*, 278. (e) Dougherty, D.; Wittel, K.; Meeks, J.; McGlynn, S. P. *J. Am. Chem. Soc.* **1976**, *98*, 3815. (f) Peng, S.; Padva, A.; LeBreton, P. R. *Proc. Natl. Acad. Sci. U.S.A.* **1976**, *73*, 2966. (g) Dougherty, D.; McGlynn, S. P. *J. Chem. Phys.* **1977**, *67*, 1289. (h) Yu, C.; Peng, S.; Akiyama, I.; Lin, J.; LeBreton, P. R. *J. Am. Chem. Soc.* **1978**, *100*, 2303. (i) Lin, J.; Yu, C.; Peng, S.; Akiyama, I.; Li, K.; Lee, L.-K.; LeBreton, P. R. *J. Phys. Chem.* **1980**, *84*, 1006. (j) Lin, J.; Yu, C.; Peng, S.; Akiyama, I.; Li, K.; Lee, L.-K.; LeBreton, P. R. *J. Am. Chem. Soc.* **1980**, *102*, 4627.

(2) (a) Padva, A.; Peng, S.; Lin, J.; Shahbaz, M.; LeBreton, P. R. *Biopolymers* **1978**, *17*, 1523. (b) Peng, S.; Lin, J.; Shahbaz, M.; LeBreton, P. R. *Int. J. Quantum Chem. Quantum Biol. Symp.* **1975**, *5*, 301.

(3) Yu, C.; O'Donnell, T. J.; LeBreton, P. R. *J. Phys. Chem.* **1981**, *85*, 3851.

(4) (a) Cowley, A. H.; Lattman, M.; Montag, R. A.; Verkade, J. G. *Inorg. Chim. Acta* **1977**, *25*, L151. (b) Chattopadhyay, S.; Findley, G. L.; McGlynn, S. P. *J. Electron Spectrosc. Relat. Phenom.* **1981**, *24*, 27. (c) LeBreton, P. R.; Fetzer, S.; Tasaki, K.; Yang, X.; Yu, M.; Slutskaya, Z.; Urano, S. *J. Biomol. Struct. Dyn.* **1988**, *6*, 199.

(5) (a) LeBreton, P. R.; Urano, S. In *Spectroscopy of Biological Molecules New Advances*; Schmid, E. D., Schneider, F. W., Siebert, F. Eds., John Wiley and Sons: Chichester, England 1988; pp 399-402. (b) Tasaki, K.; Yang; X.; Urano, S.; Fetzer, S.; LeBreton, P. R. *J. Am. Chem. Soc.*, in press.

(6) (a) Urano, S.; Fetzer, S.; Harvey, R. G.; Tasaki, K.; LeBreton, P. R. *Biochem. Biophys. Res. Commun.* **1988**, *154*, 789. (b) Geacintov, N. E. *Photochem. Photobio.* **1987**, *45*, 547. (c) Yanagida, M.; Morikawa, K.; Hiraoka, Y.; Matsumoto, S.; Uemura, T.; Okada, S. In *Applications of Fluorescence in the Biomedical Sciences*; Taylor, D. L., Waggoner, A. S., Lanni, F., Murphy, R. F., Birge, R. R., Eds.; Alan R. Liss: New York, 1986; pp 321-345. (d) Zegar, I. S.; Prakash, A. S.; Harvey, R. G.; LeBreton, P. R. *J. Am. Chem. Soc.* **1985**, *107*, 7990. (e) Abramovich, M.; Prakash, A. S.; Harvey, R. G.; Zegar, I. S.; LeBreton, P. R. *Chem. Biol. Interact.* **1985**, *55*, 39. (f) LeBreton, P. R. In *Polycyclic Hydrocarbons and Carcinogenesis*; ACS Symposium Series 283; Harvey, R. G., Ed.; American Chemical Society: Washington, DC, 1985; pp 209-238. (g) Callis, P. R. In *Annual Review of Physical Chemistry*; Rabinovitch, B. S., Schurr, J. M., Strauss, H. L., Eds.; Annual Reviews Inc.: Palo Alto, CA, 1983; Vol. 34, pp 329-357. (h) Georghiou, S. In *Modern Fluorescence Spectroscopy 3*; Wehry, E. L., Ed.; Plenum Press: New York, 1981; pp 193-249.

0002-7863/90/1512-2138$02.50/0

Table I. Crystallographic and Intensity Data Collection Parameters for 1,9-DMG and O^6,9-DMG

	1,9-DMG	O^6,9-DMG
formula	$4(C_7H_9N_5O)\cdot 1.5(CHCl_3)$	$C_7H_9N_5O$
fw, amu	4(179.18) + 1.5(119.38)	179.18
crystal class	triclinic	monoclinic
space group	$P\bar{1}(C_i^1)$	$P2_1/n(C_{2h}^5)$
dimens, mm	0.1 × 0.2 × 0.7	0.2 × 0.4 × 0.4
a, Å	13.505 (7)	10.217 (3)
b, Å	20.297 (8)	7.654 (2)
c, Å	7.632 (4)	10.722 (2)
α, deg	94.07 (2)	90
β, deg	95.20 (4)	92.09 (2)
V, Å^3	2038 (2)	837.9 (5)
z	2 (8)	4
ρ_{calcd}, g/cm^3	1.460	1.420
radiation, λ, Å	Mo Kα, 0.710 73	Mo Kα, 0.710 73
diffractometer	Syntex $P2_1$	Enraf-Nonius CAD4
octants measd	$\pm h,\pm k,+l$	$+h,+k,\pm l$
scan mode	$\omega/2\theta$, 3–14°/min	ω/θ, 2–8°/min
μ, cm^{-1}	3.84	0.97
2θ, deg	3.0–46.0	2.0–46.0
no. of measd intensities	6437	1607
no. of unique intensities	5719	1309
no. of obsd reflcns	2920 ($I > 2.58\sigma(I)$)	1075 ($I > 2.58\sigma(I)$)
R	0.087	0.034
R_w	0.101	0.039
P	0.02	0.01
$(\Delta/\sigma)_{max}$ in final cycle	0.049	0.002

bases.[13] More specifically, matrix isolation studies[13b-d] suggest that, unlike the other DNA and RNA bases, guanine nucleotides can occur in significant quantities in more than one tautomeric form, and that the populations of these different forms are strongly dependent on environment. In the present investigation, we have examined the gas-phase photoelectron and solution fluorescence properties of 1,9-dimethylguanine (1,9-DMG), O^6,9-dimethylguanine (O^6,9-DMG), and 9-methylguanine (9-MG).

In earlier photoelectron investigations of guanine from one of our laboratories,[11] it was recognized that tautomerism can complicate gas-phase spectra of nucleotide bases. The tautomer problem was partially circumvented by comparing spectral results for guanine with those for a series of methyl-substituted guanines including 7-methylguanine, 9-methylguanine, and N^2,N^2-dimethyl-9-propylguanine. Results of the investigation suggested

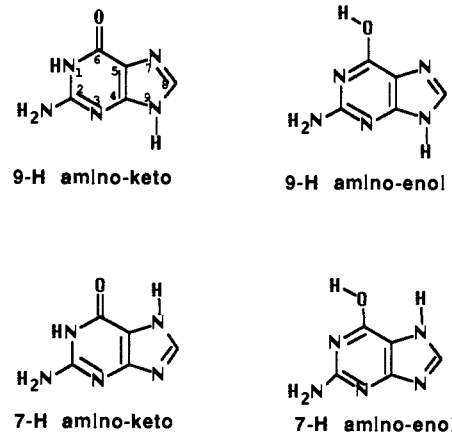

Figure 1. Structures of the 9-H and 7-H amino keto and amino enol tautomers of guanine.

Table II. Selected Average Bond Lengths and Angles for the Four Molecules/Cell of 1,9-DMG

bond	lengths (esd), Å	bond	lengths (esd), Å
N1-C2	1.38 (2)	C6-N1	1.44 (1)
C2-N2′	1.35 (1)	N1-C1′	1.48 (1)
C2-N3	1.32 (1)	C4-N9	1.36 (1)
N3-N4	1.35 (1)	N9-C9′	1.46 (1)
C4-C5	1.38 (2)	N9-C8	1.38 (1)
C5-C6	1.41 (2)	C8-N7	1.30 (1)
C6-O6′	1.23 (1)	N7-C5	1.39 (1)
atoms	**angle (esd), deg**	**atoms**	**angle (esd), deg**
N1-C2-N3	124.4 (8)	C1′-N1-C2	119.9 (7)
C2-N3-C4	112.7 (8)	C4-N9-C9′	126.6 (9)
N1-C2-N2′	117.7 (10)	C4-N9-C8	106.0 (1)
N3-C2-N2′	118.0 (1)	C8-N9-C9′	128.0 (1)
N3-C4-C5	128.7 (9)	N9-C8-N7	113.6 (9)
C4-C5-C6	119.2 (8)	C8-N7-C5	104.0 (8)
C5-C6-N1	112.0 (1)	N7-C5-C4	111.0 (1)
C5-C6-O6′	128.6 (8)	C5-C4-N9	105.8 (9)
O6′-C6-N1	120.0 (1)	N3-C4-N9	125.4 (8)
C6-N1-C2	123.4 (8)	N7-C5-C6	130.0 (1)
C6-N1-C1′	117.0 (1)		

Table III. Selected Bond Lengths and Angles for O^6,9-DMG

bond	lengths (esd), Å	bond	lengths (esd), Å
N1-C2	1.359 (2)	O6′-C6′	1.435 (2)
C2-N2′	1.354 (2)	C4-N9	1.368 (2)
C2-N3	1.337 (2)	N9-C9′	1.455 (2)
N3-C4	1.343 (2)	N9-C8	1.369 (2)
C4-C5	1.377 (2)	C8-N7	1.302 (3)
C5-C6	1.394 (2)	N7-C5	1.393 (2)
C6-O6′	1.340 (2)	N1-C6	1.319 (2)
atoms	**angle (esd), deg**	**atoms**	**angle (esd), deg**
N1-C2-N3	126.9 (1)	C6-O6′-C6′	118.1 (1)
C2-N3-C4	111.6 (1)	C4-N9-C9′	126.3 (2)
N1-C2-N2′	115.6 (1)	C4-N9-C8	105.4 (1)
N3-C2-N2′	117.5 (1)	N9-C8-N7	114.6 (2)
N3-C4-C5	127.6 (1)	C8-N7-C5	103.2 (1)
C4-C5-C6	114.7 (1)	N7-C5-C4	110.8 (1)
C5-C6-N1	121.0 (1)	N9-C4-C5	106.0 (1)
C6-N1-C2	118.2 (1)	C8-N9-C9′	128.1 (2)
C5-C6-O6′	118.8 (1)	N3-C4-N9	126.4 (1)
N1-C6-O6′	120.2 (1)	N7-C5-C6	134.5 (2)

that, in the gas phase, guanine occurs primarily in the 7-H tautomeric form.

More recent IR studies carried out in inert N_2 and Ar matrices indicate that under these special conditions guanine occurs as a mixture in which approximately 50% of the total population is in one of the 7-H tautomeric forms.[13c] When guanine is incorporated into DNA and RNA in polar environments and in crystals, it occurs in the amino keto tautomeric form.[13a] However, the recent matrix isolation experiments demonstrate that, in an inert

(7) (a) Sattsangi, P. D.; Leonard, N. J.; Frihart, C. R. *J. Org. Chem.* **1977**, *42*, 3292. (b) Secrist, J. A., III; Barrio, J. R.; Leonard, N. J.; Weber, G. *Biochemistry* **1972**, *11*, 3499. (c) Spencer, R. D.; Weber, G.; Tolman, G. L.; Barrio, J. R.; Leonard, N. J. *Eur. J. Biochem.* **1974**, *45*, 425. (d) Leonard, N. J. *C.R.C. Crit. Rev. Biochem.* **1984**, *15*, 125.

(8) Singer, B.; Grunberger, D. In *Molecular Biology of Mutagens and Carcinogens*; Plenum Press: New York, 1983; Chapter 4.

(9) Assenza, S. P.; Brown, P. R. *J. Chromatogr.* **1984**, *289*, 355.

(10) (a) Lawley, P. D.; Orr, D. J.; Jarman, M. *Biochem. J.* **1975**, *145*, 73. (b) Lawley, P. D.; Shah, S. A. *Chem. Biol. Interact.* **1973**, *7*, 115. (c) Lawley, P. D.; Thatcher, C. J. *Biochem. J.* **1970**, *116*, 693. (d) Lawley, P. D. In *Topics in Chemical Carcinogenesis*; Nakahara, W., Takayama, S., Sugimura, T., Odashima, S., Eds.; Univ. of Tokyo Press: Tokyo, 1972; pp 237–258. (e) Singer, B. *Nature* **1976**, *264*, 333. (f) Singer, B.; Fraenkel-Conrat, H. *Biochemistry* **1975**, *14*, 772. (g) Singer, B.; Bodell, W. J.; Cleaver, J. E.; Thomas, G. H.; Rajewsky, M. F.; Thon, W. *Nature* **1978**, *276*, 85. (h) Singer, B. *J. Toxicol. Environ. Health* **1977**, *2*, 1279. (i) Singer, B. In *Molecular and Cellular Mechanisms of Mutagenesis*; Lemontt, J. F., Generoso, W. M., Eds.; Plenum Press: New York, 1982; pp 1–42. (j) Pegg, A. E.; Singer, B. *Cancer Invest.* **1984**, *2*, 221.

(11) Singer, B. *J. Natl. Cancer Inst.* **1979**, *62*, 1329.

(12) (a) Warren, W.; Lawley, P. D. *Carcinogenesis* **1980**, *1*, 67. (b) Singer, B.; Spengler, S.; Bodell, W. J. *Carcinogenesis* **1981**, *2*, 1069. (c) Den Engelse, Menkveld, G. J.; Debrij, R.-J.; Tates, A. D. *Carcinogenesis* **1986**, *7*, 393. (d) Singer, B.; Brent, T. P. *Proc. Natl. Acad. Sci. U.S.A.* **1981**, *78*, 856. (e) Pegg, A. E. *Rev. Biochem. Toxicol.* **1983**, *5*, 83–133.

(13) (a) Sanger, W. *Principles of Nucleic Acid Structure*, Springer: Berlin, 1984; pp 110 ff, and references therein. (b) Szczepaniak, K.; Szczesniak, M.; Person, W. B. *Int. J. Quantum Chem. Quantum Biol. Symp.* **1986**, *13*, 287. (c) Szczepaniak, K.; Szczesniak, M. *J. Mol. Struct.* **1987**, *156*, 29. (d) Szczepaniak, K.; Szczesniak, M.; Person, W. B. *Chem. Phys. Lett.* **1988**, *153*, 39.

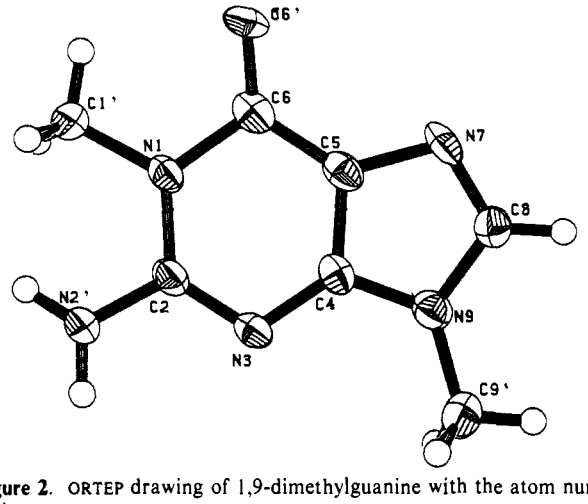

Figure 2. ORTEP drawing of 1,9-dimethylguanine with the atom numbering.

environment, guanine participates in a tautomeric equilibrium that involves amino enol and amino keto structures. For guanine[13c] and 9-methylguanine,[13d] amino enol tautomeric forms make up 67% and 50% of the total populations, respectively. Figure 1 shows 9-H and 7-H, amino enol and amino keto structures of guanine.

One goal of the present investigation has been to employ UV photoelectron spectroscopy, and ab initio quantum mechanical calculations with the 3-21G and 4-31G basis sets, as well as semiempirical HAM/3 calculations to provide descriptions of the valence electronic structures of guanine. Here methyl substitution has been used to restrict the formation of equilibrium mixtures of tautomers. X-ray data have been measured for 1,9-DMG and O^6,9-DMG in order to obtain geometric parameters used in the quantum mechanical calculations. This investigation, which focuses on 1,9-DMG, O^6,9-DMG, and 9-MG, elucidates the ground-state electronic structure of guanine that occurs naturally in DNA and RNA, and the electronic structure of modified guanine, which has genotoxic properties.

A second goal has been to employ fluorescence emission and fluorescence lifetime measurements and results from HAM/3 and CNDO/S semiempirical CI calculations to compare the fluorescence properties of 1,9-DMG, O^6,9-DMG, and 9-MG at low pH.

Results

Crystallographic Structures. Table I gives the crystallographic and intensity X-ray data collection parameters and Tables II and III give the bond lengths and bond angles obtained from X-ray data for 1,9-DMG and O^6,9-DMG. Figures 2 and 3 provide ORTEP drawings representative of 1,9-DMG and O^6,9-DMG structures, and Figure 4 depicts the unit cell of 1,9-DMG with hydrogen bonding.

Photoelectron Spectra. Figure 5 shows photoelectron spectra and assignments for 1,9-DMG, O^6,9-DMG, and 9-MG. In all three spectra the first photoelectron band is well resolved. All of the first vertical ionization potentials (IPs) lie in the range 7.9–8.2 eV. The spectra of 9-MG and O^6,9-DMG are similar in the energy range 7.5–11.8 eV. In the spectra of both molecules this energy range contains a broad region of high photoelectron intensity that exhibits five maxima. In O^6,9-DMG they occur at 7.96, 9.2, 10.0, 10.6, and 11.29 eV. In the energy region 7.5–11.8 eV, the spectrum of 1,9-DMG is different from the spectra of 9-MG and O^6,9-DMG. In the spectrum of 1,9-DMG, the energy region from 7.5 to 11.8 eV contains only four maxima. These occur at 8.09, 9.5, 10.0, and 11.0 eV.

Assignment of Photoelectron Spectra. As an aid in interpreting the spectra, quantum mechanical calculations have been carried out using the semiempirical HAM/3 method.[14] The HAM/3 calculations were run on an IBM 3090-120E computer. The spectra have also been assigned by applying Koopmans' theorem[15] to results from ab initio SCF molecular orbital calculations employing the 3-21G[16] and 4-31G[17] basis sets. The ab initio calculations were carried out on CRAY X-MP/48 and IBM 3090/600 VF computers using the GAUSSIAN 86 program.[18]

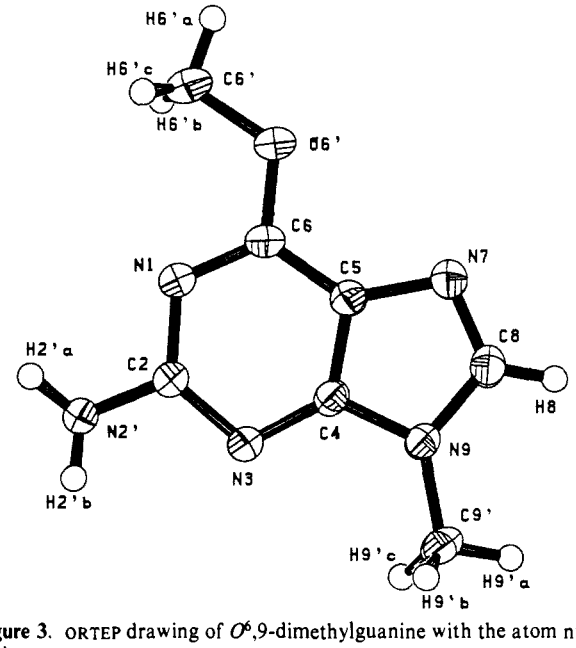

Figure 3. ORTEP drawing of O^6,9-dimethylguanine with the atom numbering.

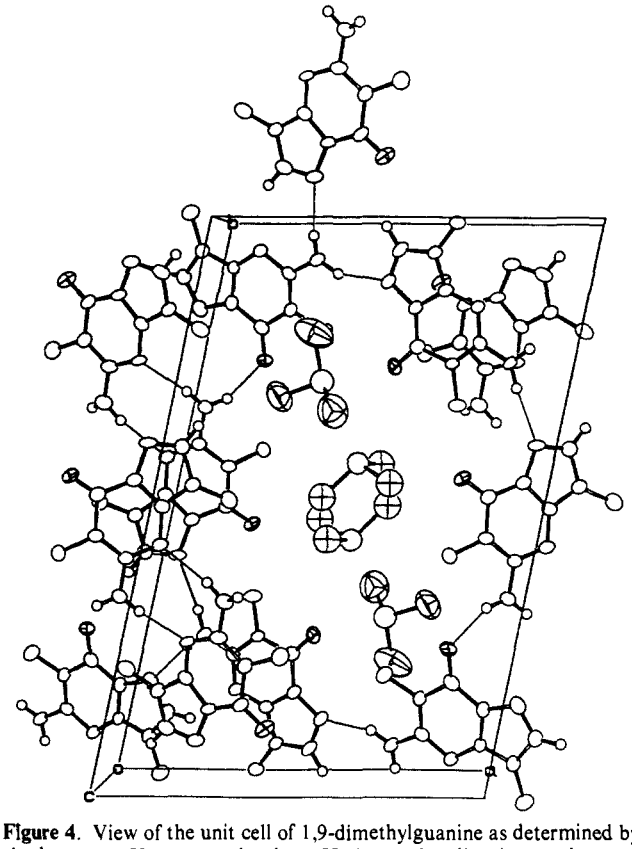

Figure 4. View of the unit cell of 1,9-dimethylguanine as determined by single-crystal X-ray examination. Hydrogen-bonding interactions are indicated.

(14) (a) Asbrink, L.; Fridh, C.; Lindholm, E. *Chem. Phys. Lett.* **1977**, *52*, 63. (b) Åsbrink, L.; Fridh, C.; Lindholm, E. *Ibid.* **1977**, *52*, 69. (c) Åsbrink, L.; Fridh, C.; Lindholm, E. *Tetrahedron Lett.* **1977**, *19*, 4627.

(15) Koopmans, T. *Physica* **1933**, *1*, 104.

(16) Binkley, J. S.; Pople, J. A.; Hehre, W. J. *J. Am. Chem. Soc.* **1980**, *102*, 939.

(17) Ditchfield, R.; Hehre, W. J.; Pople, J. A. *J. Chem. Phys.* **1971**, *54*, 724.

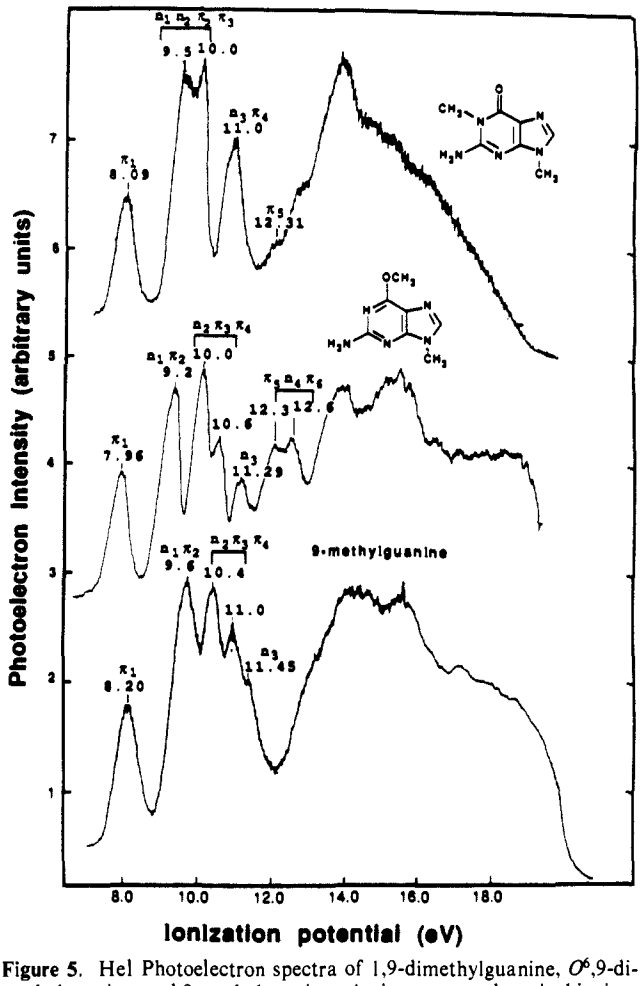

Figure 5. Hel Photoelectron spectra of 1,9-dimethylguanine, O^6,9-dimethylguanine, and 9-methylguanine. Assignments and vertical ionization potentials are also given.

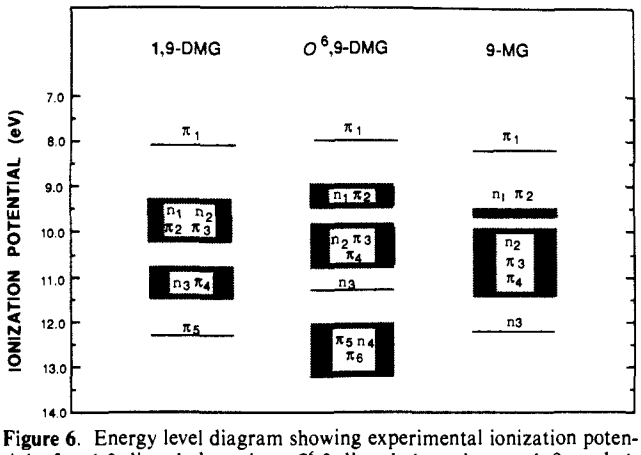

Figure 6. Energy level diagram showing experimental ionization potentials for 1,9-dimethylguanine, O^6,9-dimethylguanine, and 9-methylguanine.

Results from the 4-31G SCF calculations have also been used to construct diagrams of valence orbitals in 1,9-DMG and O^6,9-DMG.[4c,19]

For the calculations, geometries of 1,9-DMG and O^6,9-DMG were taken directly from crystallographic data. For calculations

(18) The GAUSSIAN 86 program was obtained from Carnegie Mellon University and written by J. Stephen Binkley, Michael Frisch, Krishnan Raghavachavi, Douglas DeFrees, H. Bernhard Schlegel, Robert Whiteside, Eugene Fluder, Rolf Seeger, Douglas J. Fox, Martin Head-Gordon, and Sid Topiol.

(19) Kimura, K.; Katsumata, S.; Achiba, Y.; Yamazaki, T.; Iwata, S. *Handbook of Hel Photoelectron Spectra of Fundamental Organic Molecules*; Halsted Press: New York, 1981; p 20.

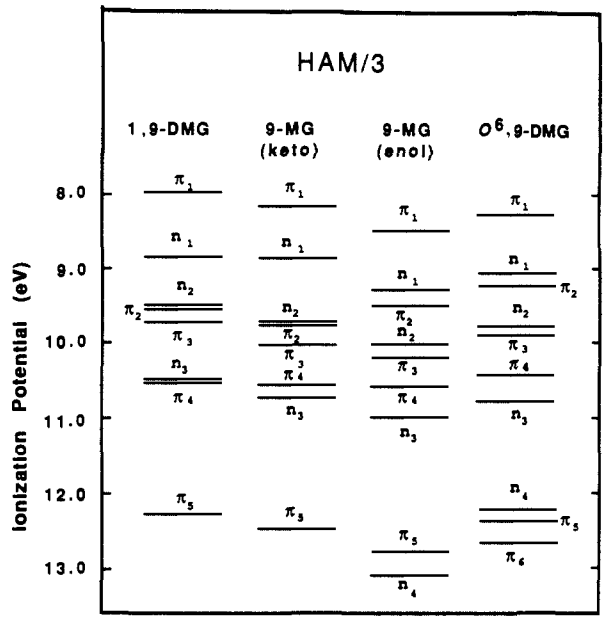

Figure 7. Energy level diagram showing theoretical ionization potentials of 1,9-dimethylguanine, O^6,9-dimethylguanine, and 9-methylguanine obtained from HAM/3 calculations. For 9-methylguanine, energy levels are given for both the amino enol and amino keto tautomers. The diagram gives ionization potentials of the orbitals that are assigned in the spectra contained in Figure 5.

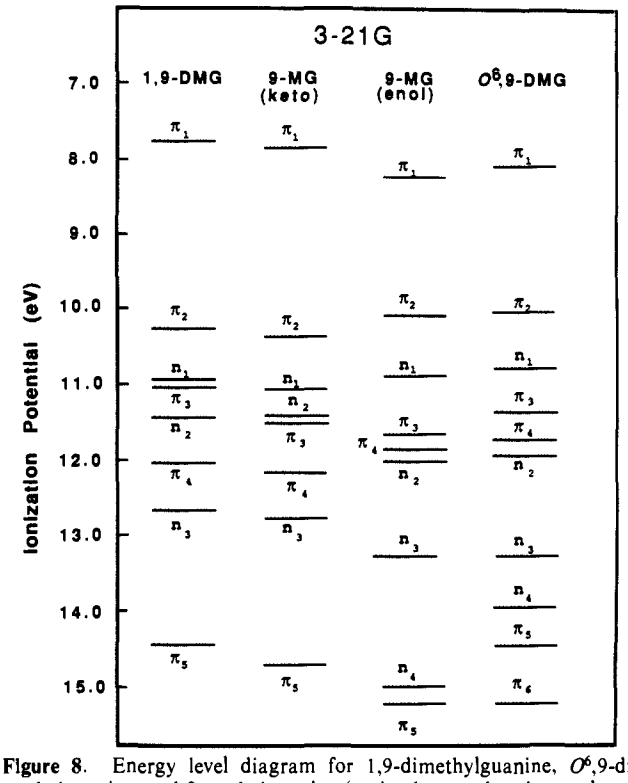

Figure 8. Energy level diagram for 1,9-dimethylguanine, O^6,9-dimethylguanine, and 9-methylguanine (amino keto and amino enol tautomers) obtained from 3-21G calculations.

on 9-MG in the amino enol and amino keto tautomeric forms, the geometries were based upon those of O^6,9-DMG and 1,9-DMG.

Figure 6 shows experimental vertical IPs for 1,9-DMG, O^6,9-DMG, and 9-MG. Figures 7–9 show theoretical IPs obtained from the results of semiempirical HAM/3 and ab initio 3-21G and 4-31G calculations. For all three molecules, all of the calculations predict that the highest occupied molecular orbital is a π orbital.

Semiempirical HAM/3 Calculations. Figure 7 summarizes results of the HAM/3 calculations on 1,9-DMG, O^6,9-DMG, and 9-MG, in the amino keto and amino enol tautomeric forms. The

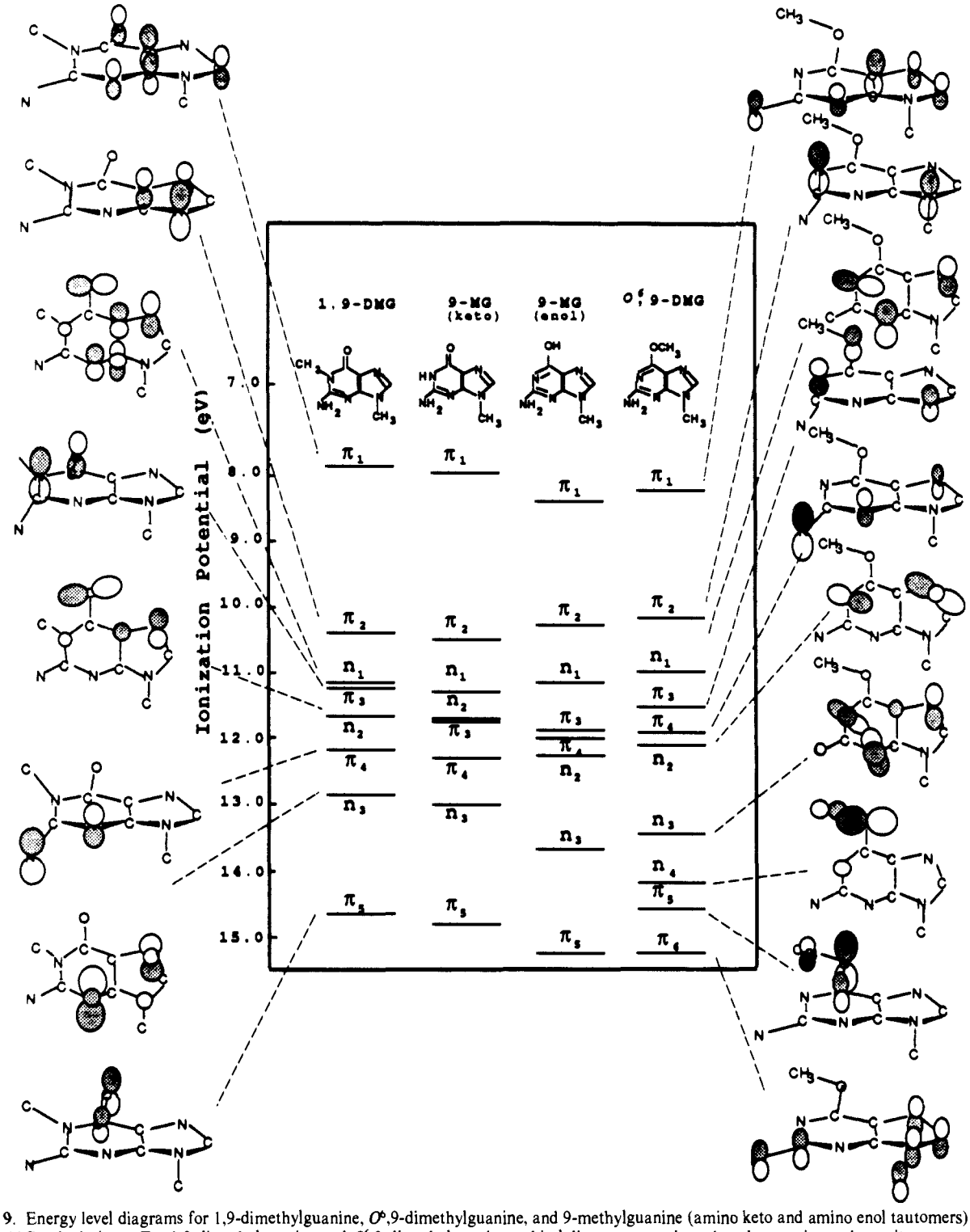

Figure 9. Energy level diagrams for 1,9-dimethylguanine, O^6,9-dimethylguanine, and 9-methylguanine (amino keto and amino enol tautomers) obtained from 4-31G calculations. For 1,9-dimethylguanine and O^6,9-dimethylguanine, orbital diagrams are given that show major carbon, nitrogen, and oxygen 2s and 2p contributions to the upper occupied π and lone-pair orbitals for which assignments are given in Figure 5. In each molecular orbital all C, N, and O 2p contributions are shown for which inner orbital coefficients are greater than 0.20. All 2s contributions are shown for which outer orbital coefficients are greater than 0.20. See ref 19.

results in Figure 7 demonstrate that for 1,9-DMG and O^6,9-DMG, which exist in only one tautomeric form, the HAM/3 calculations reproduce the pattern of energy levels observed in the photoelectron spectra.

For 1,9-DMG, the vertical IP of the highest occupied π_1 orbital is 8.09 eV. The IP predicted by the HAM/3 calculations is 8.05 eV. According to the HAM/3 results for 1,9-DMG, the energy region between 8.83 and 9.71 eV contains four bands arising from two lone-pair orbitals (n_1 and n_2) and two π orbitals (π_2 and π_3). In Figure 5, these four bands have been assigned to the energy region between 9.3 and 10.2 eV. The HAM/3 calculations predict that the n_3 and π_4 orbitals have IPs of 10.46 and 10.52 eV. Bands arising from these orbitals have been assigned to the energy region containing a maximum at 11.0 eV. The band that appears at 12.31 eV has been assigned to the π_5 orbital. The HAM/3 results predict that this orbital has an IP of 12.25 eV.

For O^6,9-DMG, the HAM/3 results indicate that the value of the first π ionization potential is 8.24 eV. The experimental value is 7.96 eV. The emission maximum in the spectrum of O^6,9-DMG, which occurs at 9.2 eV, has been assigned to the n_1 and π_2 orbitals. According to the HAM/3 results, the IPs of these orbitals are 9.04 and 9.24 eV. The energy region between 9.8 and 10.7 eV

in the spectrum of O^6,9-DMG has been assigned to the n_2, π_3, and π_4 orbitals. The HAM/3 results predict that the IPs of these orbitals are 9.75, 9.88, and 10.37 eV, respectively. The band appearing at 11.29 eV in the spectrum of O^6,9-DMG has been assigned to the n_3 orbital. The HAM/3 calculations predict that this orbital has an IP of 10.73 eV. The bands in the energy region between 12.1 and 12.7 eV, which give rise to two broad maxima in the spectrum of O^6,9-DMG, have been assigned to the n_4, π_5, and π_6 orbitals. According to the HAM/3 results, the IPs of these orbitals are 12.20, 12.33, and 12.66 eV, respectively.

In Figure 7, the energy level diagram for the amino keto tautomer of 9-DMG is similar to that of 1,9-DMG, while the energy level diagram for the amino enol tautomer of 9-MG is similar to that for O^6,9-DMG. The introduction of methyl groups causes a lowering of valence orbital IPs in both tautomers. For the amino enol tautomer of 9-MG, results of the HAM/3 calculations predict that the energetic ordering of π_5 and n_4 orbitals is reversed compared to that in O^6,9-DMG.

Ab Initio 3-21G and 4-31G SCF Calculations. Figure 8 shows valence orbital energies for 1,9-DMG, 9-MG, and O^6,9-DMG obtained from results of 3-21G SCF calculations. Figure 9 contains energy levels and orbital diagrams obtained from results of 4-31G calculations.

The absolute values for the π_1 ionization potentials obtained from 3-21G and 4-31G calculations are of approximately the same accuracy as the values obtained from HAM/3 calculations. For 1,9-DMG and O^6,9-DMG, both the ab initio and the semiempirical results agree with experiment to within 0.35 eV. For the second through eighth highest occupied orbitals in 1,9-DMG, and for the second through tenth orbitals in O^6,9-DMG, the 3-21G and 4-31G calculations are less accurate than the HAM/3 calculations. Here the ab initio calculations predict IPs that are 0.8–2.5 eV higher than the experimental values. For these orbitals, the HAM/3 values agree with experiment to within 0.7 eV.

For 1,9-DMG, both the 3-21G and the 4-31G calculations predict the same energetic ordering of the upper occupied orbitals. In some cases where orbital energy differences are small, this ordering is different from that predicted by the HAM/3 calculations. Nevertheless, the patterns of energy levels obtained from the HAM/3 and ab initio calculations are similar, and in this sense, the assignments given in Figure 5 are in agreement with both types of calculations. According to the ab initio results, the ordering of the second through the eighth orbitals in 1,9-DMG is π_2, n_1, π_3, n_2, π_4, n_3, and π_5. In Figure 5, the assignment of the first four of these orbitals to the broad emission occurring between 9.3 and 10.2 eV agrees with the pattern of the ab initio results. Also consistent with the ab initio results is the assignment of the π_4 and n_3 orbitals to the emission peaking at 11.0 eV. Finally, the pattern of the ab initio results agrees with the assignment of the π_5 orbital to the band at 12.31 eV.

As in 1,9-DMG, the energetic ordering of the upper occupied orbitals in O^6,9-DMG predicted by 3-21G calculations is identical with that predicted by 4-31G calculations. For closely spaced orbitals, the ab initio calculations again provide a slightly different energetic ordering than the HAM/3 calculations. However, the assignment of the spectrum of O^6,9-DMG, given in Figure 5, is consistent with the ab initio results. The ab initio calculations predict that the second through sixth highest occupied orbitals in O^6,9-DMG occur in the order π_2, n_1, π_3, π_4, and n_2. In Figure 5, the first two of these orbitals have been assigned to the emission with a maximum at 9.2 eV, while the remaining three orbitals have been assigned to the emission located between 9.8 and 10.7 eV. Similarly, the assignment of the n_3 orbital to the band at 11.29 eV, and the n_4, π_5, and π_6 orbitals to the photoelectron envelope located between 12.1 and 12.7 eV is consistent with the ab initio results.

As with the HAM/3 calculations, both the 3-21G and the 4-31G calculations predict that methylation of the amino keto and amino enol tautomers of 9-MG causes destabilization of the upper occupied valence orbitals. The results of both ab initio calculations indicate that N1 methylation of the amino keto tautomer causes a reverse in the energetic ordering of the n_2 and π_3 orbitals. For the amino enol tautomer of 9-MG, the 3-21G calculations predict an ordering of the n_4 and π_5 orbitals different from that obtained from the 4-31G calculations. The 4-31G calculations indicate that the n_4 orbital has an IP 0.12 eV higher than that of the π_5 orbital.

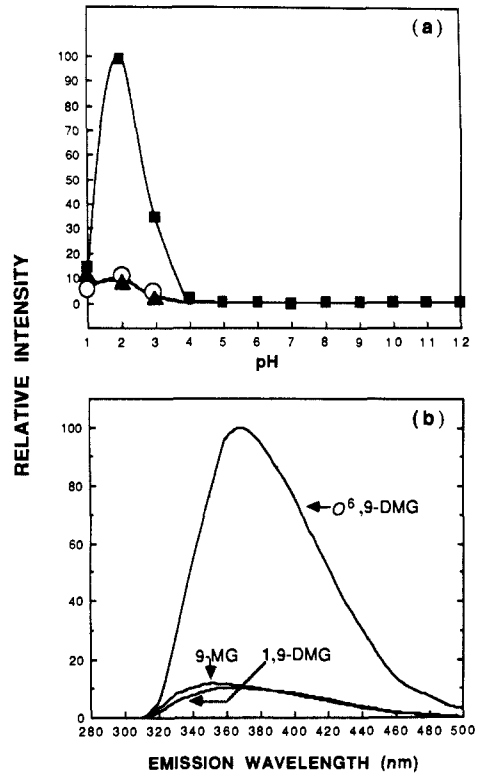

Figure 10. (a) Relative fluorescence intensities of 1,9-dimethylguanine (▲), O^6,9-dimethylguanine (■), and 9-methylguanine (○) as a function of pH. (b) Corrected fluorescence emission spectra of 1,9-dimethylguanine, O^6,9-dimethylguanine, and 9-methylguanine measured at a pH of 2.0.

Fluorescence Measurements. Figure 10a illustrates the pH dependence of the fluorescence emission intensities of 1,9-DMG, O^6,9-DMG, and 9-MG, at an excitation wavelength of 270 nm. The emission wavelengths were 400 nm for 1,9-DMG and 390 nm for O^6,9-DMG and 9-MG. Both emission wavelengths correspond to the maxima in the corrected emission spectra measured at a pH of 7.1. As demonstrated in Figure 10a, the maximum fluorescence intensities for O^6,9-DMG, 1,9-DMG, and 9-MG occur at a pH of 2.0 where all three compounds are protonated. For O^6,9-DMG, the fluorescence intensity data indicate that emission is associated with a species having a pK_a of $\approx$2.7. This is similar to the reported value of 3.0 for the pK_a of guanine.[20] Figure 10b shows corrected fluorescence emission spectra of 1,9-DMG, O^6,9-DMG, and 9-MG measured at an excitation wavelength of 270 nm and at a pH of 2.0.

The results in Figure 10b indicate that O^6,9-DMG exhibits an integrated intensity that is 11.0 and 9.2 times greater than the intensities of 1,9-DMG and 9-MG. A comparison of the extinction coefficients of the three cations at 270 nm indicates that the value of O^6,9-DMG is 28% lower than the values for 1,9-DMG and 9-MG, which demonstrates that the higher fluorescence emission intensity of O^6,9-DMG is due to a greater fluorescence quantum yield.

Figure 11 shows fluorescence decay profiles of 1,9-DMG, O^6,9-DMG, and 9-MG measured at a pH of 2.0. The excitation wavelength used for all of the compounds was 270 nm, and the emission wavelengths were 375 nm for 1,9-DMG and O^6,9-DMG and 365 nm for 9-MG. These emission wavelengths correspond to the maxima in the emission spectra measured at a pH of 2.0.

(20) Albert, A. In *Physical Methods in Heterocyclic Chemistry*; Katritzky, A. R., Ed.; Academic Press: New York, 1963; Vol. I, p 101.

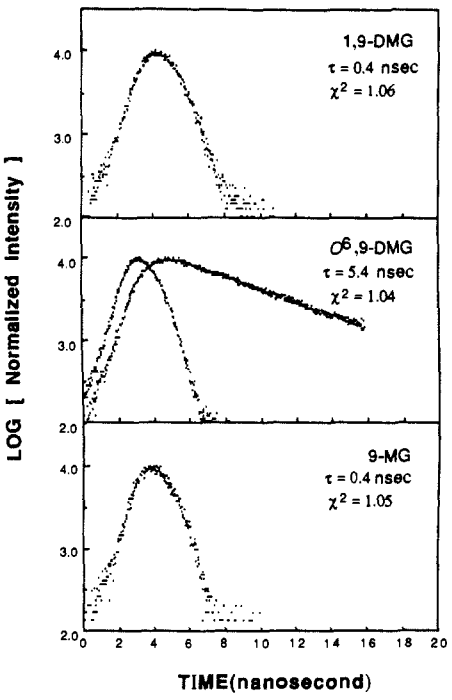

Figure 11. Fluorescence decay profiles of 1,9-dimethylguanine, O^6,9-dimethylguanine, and 9-methylguanine, measured at a pH of 2.0 along with lifetime and χ^2 values obtained from deconvolution of the data. In addition to the data for O^6,9-dimethylguanine, the middle panel of the figure contains an instrument response profile.

For all of the compounds investigated here, a single-exponential decay law was sufficient to obtain a good fit to the experimental decay profiles. No improvements in the χ^2 values were obtained when a double-exponential decay law was employed. Fluorescence lifetimes (τ) of 5.4, 0.4, and 0.4 ns were obtained for O^6,9-DMG, 1,9-DMG, and 9-MG, respectively. The uncertainty in the measured lifetimes is ±0.1 ns.

Discussion

Assignment of the Photoelectron Spectra of Methyl-Substituted Guanines and Gas-Phase Tautomerism of 9-Methylguanine. The assignments of the photoelectron spectra of 1,9-DMG and O^6,9-DMG are consistent with results from semiempirical HAM/3 calculations and ab initio SCF calculations employing the 3-21G and 4-31G basis sets. In all cases where discrepancies occur in the energetic ordering of orbitals predicted by the different calculations, the spectra exhibit an overlapping of photoelectron bands. This indicates that, in cases where different computational methods yield different predictions concerning the energetic ordering of orbitals, the experimental ionization potentials of the orbitals in question are nearly equal.

The assignments of the spectra are also consistent with the observed intensities given in Figure 5. For example, the integrated intensity of the broad envelope occurring between 9.3 and 10.2 eV in the spectrum of 1,9-DMG, which has been assigned to four bands, is approximately 4 times greater than the intensity associated with the π_1 band occurring at 8.09 eV. Similarly, the intense maximum in the spectrum of O^6,9-DMG, which occurs at 9.2 eV, has been assigned to two bands, while the emission occurring between 9.8 and 10.7 eV, which contains two maxima, one intense and one weak, has been assigned to three bands. At IPs above 11.0 eV, the weaker intensities associated with overlapping bands are due to a reduction in the spectrometer transmission efficiency, which occurs as the photoelectron kinetic energy decreases.

9-Methylguanine. For 9-MG, the question of tautomerism complicates the assignment of the spectrum. Furthermore, the computational results of all three theoretical approaches employed indicate that the differences in the ionization potentials of corresponding orbitals in the two tautomers are less than 0.6 eV. However, a direct examination of the spectra in Figure 5 permits a conjecture concerning the tautomeric makeup of 9-MG in the gas phase. Specifically, the observation of five maxima in the spectra of both 9-MG and O^6,9-DMG in the energy range 7.5–11.8 eV and the observation of only four maxima in the corresponding energy region of the spectrum of 1,9-DMG support the conclusion that the amino enol tautomeric form of 9-MG predominates.

The assignment of the spectrum of 9-MG in Figure 5 is based on this observation and is consistent with IPs computed for the amino enol tautomer. According to the results from the HAM/3, 3-21G, and 4-31G calculations, the first IP of 9-MG, which has a value of 8.20 eV, arises from a π orbital. All of the calculations yield values of this IP that agree with experiment to within 0.28 eV. The HAM/3 calculation and the two ab initio calculations predict different energetic orderings for orbitals that give rise to emission occurring between 9.4 and 11.7 eV. However, results from both the semiempirical and the ab initio calculations are consistent with the assignment of the n_1 and π_2 orbitals to the envelope with a maximum at 9.6 eV. Similarly, results from the semiempirical and ab initio calculations are consistent with the assignment of the n_2, π_3, and π_4 orbitals to the energy region containing the maxima occurring at 10.4 and 11.0 eV. According to the ab initio calculations, the emission with a maximum at 10.4 eV contains bands arising from the n_2 and π_3 orbitals. According to the HAM/3 calculations, this region contains bands arising from the π_3 and π_4 orbitals. Because of this discrepancy, a precise assignment of the n_2, π_3, and π_4 orbitals is not possible at this time. While the ab initio and semiempirical calculations yield different predictions concerning the assignments of the n_2, π_3, and π_4 orbitals, results from both types of calculations are consistent with the assignment of the n_3 orbital to the shoulder located at 11.45 eV.

The present results suggest that the amino enol tautomer of 9-MG predominates. However, it is probable that a significant amount of the amino keto tautomer is also present. The possibility that a mixture of tautomers occurs under our experimental conditions is indicated by the resolution of the spectrum of 9-MG in Figure 5. In the energy region between 8.9 and 11.0 eV, the spectrum of 9-MG contains no low minima corresponding to that occurring at 9.7 eV in the spectrum of O^6,9-DMG, or to that occurring at 10.6 eV in the spectrum of 1,9-DMG. This lack of any interval of low intensity in the energy region containing a large number of bands is expected if more than one species is contributing to the observed spectrum.

The possibility that a mixture of tautomers contributes to the spectrum of 9-MG is consistent with data from the matrix isolation experiments indicating that the population is 50% in the amino enol form and 50% in the amino keto form.[13c] It should be further noted that the present photoelectron investigation does not exclude the possibility of contributions from other exotic forms of 9-MG such as the exo imino enol tautomer. However, to date, we have found no reported evidence for such alternate tautomers.

Fluorescence Properties of 1,9-DMG, O^6,9-DMG, and 9-MG. Consistent with previous fluorescence studies of the products of DNA and RNA alkylation reactions, our results indicate that O^6,9-DMG has a higher fluorescence quantum yield than 1,9-DMG.[8,9] Other investigations have demonstrated that the significant increase in the fluorescence quantum yield of guanine, which O^6 methylation induces at low pH, permits, under favorable spectroscopic conditions, the detection of O^6-alkylated guanine in the presence of unmodified guanine in ratios as low as 1 in 25 000.[8]

At an excitation wavelength of 270 nm, the greatest difference in the integrated fluorescence intensities of O^6,9-DMG compared with 1,9-DMG was observed at a pH of 2.0. As expected, the fluorescence lifetime of 1,9-DMG (0.4 ns) is less than that of O^6,9-DMG (5.4 ns). At low pH, the fluorescence properties of 1,9-DMG and 9-MG are nearly the same. At a pH of 2.0, the ratio of the integrated emission intensities for 1,9-DMG and 9-MG is 1:1.2, and the fluorescence lifetimes are equal within experimental error. The similarities between the fluorescence properties of 9-MG and 1,9-DMG suggest that in aqueous solution analogous protonated forms of the two molecules are responsible for the observed emission.

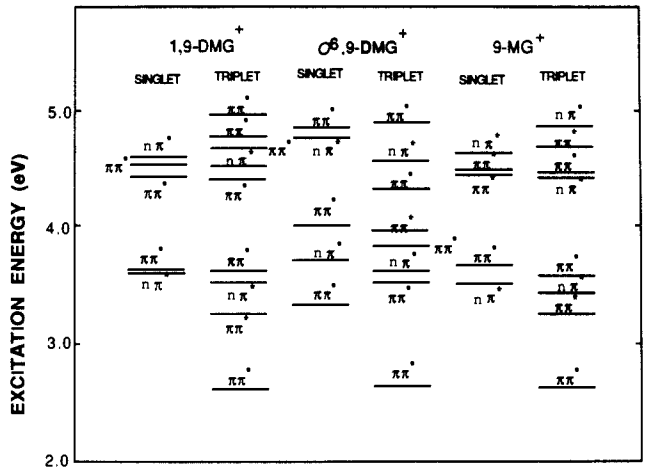

Figure 12. Energy level diagram, obtained from HAM/3 CI calculations, showing singlet and triplet excited states of N7-protonated 1,9-dimethylguanine, O^6,9-dimethylguanine, and 9-methylguanine.

One mechanism that may explain the low fluorescence quantum yields of protonated 1,9-DMG and 9-MG versus O^6,9-DMG is based on a proximity effect that becomes important as the energy difference between the lowest excited singlet $\pi\pi^*$ and $n\pi^*$ states becomes small.[21] For molecules in which the first excited singlet state (S_1) is $\pi\pi^*$ this mechanism relies upon the observation that internal conversion to the ground singlet state (S_0) is efficiently mediated by the second excited singlet state (S_2), when the S_2 state has $n\pi^*$ symmetry and an energy almost equal to that of the S_1 state. Internal conversion is also efficient if the S_1 state is $n\pi^*$ and the S_2 state is $\pi\pi^*$. The radiationless transitions occur via vibronic coupling involving out-of-plane vibrations.[21]

An alternate mechanism, which may also explain the low fluorescence quantum yields of 1,9-DMG and 9-MG compared with O^6,9-DMG, depends upon the occurrence of an $n\pi^*$ triplet state with an energy approximately equal to that of a $\pi\pi^*$ S_1 state, or of a $\pi\pi^*$ triplet state with energy approximately equal to that of an $n\pi^*$ S_1 state. This mechanism is based upon the general observation (El-Sayed's rule) that, when the singlet–triplet energy difference is small, $\pi\pi^* \rightarrow n\pi^*$ and $n\pi^* \rightarrow \pi\pi^*$, singlet to triplet intersystem crossing occurs efficiently.[22]

In order to assess the potential importance of these two quenching mechanisms, the low-lying excited singlet and triplet electronic states of protonated 1,9-DMG, 9-MG, and O^6,9-DMG were examined by using results from HAM/3 CI calculations. The calculations were carried out on the N7-protonated cations. The N7 position of guanine is the most basic as indicated by the observations that N7 protonation occurs in the 5′-GMP zwitterion[23] and that the pK_a of 1-methylimidazole (7.25) is significantly larger than the pK_a of pyrimidine (1.3).[24] In the HAM/3 calculations, the amino keto form of N7-protonated 9-MG was examined because of the similarities observed between the low pH fluorescence properties of 1,9-DMG and 9-MG.

For the calculations on N7-protonated 1,9-DMG and 9-MG, geometries were obtained from crystallographic data for the 5′-GMP zwitterion.[23] The C–N bond lengths used for the methyl groups were obtained from the corresponding neutral molecules. The geometry for N7-protonated O^6,9-DMG was obtained by combining the geometry of the imidazole ring, used in calculations on 1,9-DMG and 9-MG, with the geometry of the pyrimidine ring in neutral O^6,9-DMG.

Figure 12 shows calculated excitation energies of the N7-protonated methylated guanines. The HAM/3 CI results in Figure 12 suggest that, because of a better matching between the S_1 and the triplet state energies, more favorable intersystem crossing occurs in 1,9-DMG and 9-MG that in O^6,9-DMG. This may contribute to the lower fluorescence quantum yields of 1,9-DMG and 9-MG. According to the results of the HAM/3 CI calculations, the energy differences between the S_1 state and the triplet state to which efficient intersystem crossing is expected are 104 and 480 cm^{-1} for 1,9-DMG and 9-MG, respectively. For O^6,9-DMG, the corresponding energy difference is 2378 cm^{-1}.

The potential importance of intersystem crossing as a source of the low fluorescence quantum yields of protonated 1,9-DMG and 9-MG, compared to O^6,9-DMG, is also indicated by results obtained from supplementary CNDO/S CI calculations,[25] using the Mataga integrals.[26] Like the HAM/3 results, the CNDO/S results indicate that the energy differences between the S_1 states and the triplet states of favorable symmetry are smaller for 1,9-DMG (1232 cm^{-1}) and 9-MG (1194 cm^{-1}) than for O^6,9-DMG (4367 cm^{-1}).

While both the HAM/3 and the CNDO/S results suggest that intersystem crossing may quench the fluorescence of protonated 1,9-DMG and 9-MG, a clear-cut assessment of the importance of this mechanism is complicated when the energies of the S_1 and S_2 states are nearly equal, causing uncertainty in the identity of the S_1 state. In 1,9-DMG and 9-MG, the S_1 and S_2 states are closely spaced and this uncertainty occurs. It is demonstrated by the HAM/3 and CNDO/S results. The HAM/3 calculations predict that in these cations the S_1 states are $n\pi^*$, while the CNDO/S calculations predict the S_1 states are $\pi\pi^*$.

The small energy differences between the S_1 and S_2 states of protonated 1,9-DMG and 9-MG, predicted by the semiempirical calculations, provide evidence that the proximity effect plays a role in limiting the fluorescence quantum yields of these cations. According to the HAM/3 results, one of the two lowest excited singlet states in 1,9-DMG, 9-MG, and O^6,9-DMG is a $\pi\pi^*$ state, and the other is an $n\pi^*$ state. The results also indicate that the energy differences between the lowest lying $\pi\pi^*$ and $n\pi^*$ states in 1,9-DMG (123 cm^{-1}) and 9-MG (1165 cm^{-1}) are smaller than in O^6,9-DMG (2971 cm^{-1}).

As with the HAM/3 results, the CNDO/S results predict that in all three cations one of the two lowest excited singlet states is a $\pi\pi^*$ state, and the other is an $n\pi^*$ state. Also, the CNDO/S results indicate that the energy differences between the S_1 and S_2 states in 1,9-DMG (1232 cm^{-1}) and 9-MG (1195 cm^{-1}) are smaller than in O^6,9-DMG (4365 cm^{-1}).

Furthermore, the smaller energy differences between the S_1 and S_2 states in 1,9-DMG and 9-MG compared to O^6,9-DMG, which are predicted by the semiempirical calculations, are not strongly dependent upon the geometries employed. For example, when geometries of protonated 1,9-DMG, 9-MG, and O^6,9-DMG were used in which the ring structures were taken to be the same as those in the corresponding neutral molecules and the N7–H^+ bond length was taken to be 1.00 Å, similar results were obtained. For each cation, the HAM/3 and CNDO/S calculations predict that one of the two lowest singlet excited states is $\pi\pi^*$, while the other is $n\pi^*$. According to the HAM/3 calculations, the energy differences between the S_1 and S_2 states in 1,9-DMG (1400 cm^{-1}) and 9-MG (320 cm^{-1}) are again smaller than in O^6,9-DMG (2940 cm^{-1}). The same trend was obtained from the results of CNDO/S calculations. Here the energy differences between the S_1 and S_2 states of 1,9-DMG, 9-MG, and O^6,9-DMG are predicted to be 1850, 600, and 4910 cm^{-1}, respectively.

The magnitudes of the energy gaps between the S_1 and S_2 states, which are predicted by the HAM/3 and CNDO/S calculations, are also in a range where S_1–S_2 vibronic coupling is expected to be significant. In gas-phase isoquinoline, where the proximity

(21) (a) Lim, E. C. *J. Phys. Chem.* **1986**, *90*, 6770. (b) Wassam, W. A., Jr.; Lim, E. C. *Chem. Phys.* **1980**, *48*, 299. (c) Lai, T.-I.; Lim, E. C. *J. Am. Chem. Soc.* **1985**, *107*, 1134.

(22) (a) El-Sayed, M. A. *J. Chem. Phys.* **1963**, *38*, 2834. (b) Hirayama, S. *J. Chem. Soc., Faraday Trans. 1* **1982**, *78*, 2411. (c) Matsumoto, T.; Sato, M.; Hirayama, S. *Chem. Phys. Lett.* **1972**, *13*, 13. (d) Mitchell, D. J.; Schuster, G. B.; Drinkamer, H. G. *J. Am. Chem. Soc.* **1977**, *99*, 1145.

(23) Emerson, J.; Sundaralingam, M. *Acta Crystallogr.* **1980**, *B36*, 1510.

(24) (a) Hofmann, K. *Imidazole and Its Derivatives*; Interscience: New York, 1953; Part 1, p 15. (b) Brown, D. J.; Masson, S. F. *The Pyrimidines*; Interscience: New York, 1962; pp 472–476.

(25) (a) Del Bene, J.; Jaffe, H. H. *J. Chem. Phys.* **1968**, *48*, 1807. (b) *Ibid.* **1968**, *48*, 4050. (c) *Ibid.* **1968**, *49*, 1221. (d) *Ibid.* **1969**, *50*, 1126. (e) Ellis, R. L.; Kuehnlenz, G.; Jaffe, H. H. *Theor. Chim. Acta* **1972**, *26*, 131.

(26) Nishimoto, K.; Mataga, N. *Z. Phys. Chem.* **1957**, *12*, 335.

effect efficiently quenches fluorescence, the energy gap between S_1 ($\pi\pi^*$) and S_2 ($n\pi^*$) is approximately 1100 cm^{-1}.[21a]

In conclusion, the results of HAM/3 and CNDO/S calculations support the notion that the proximity effect plays a significant role in reducing the fluorescence quantum yields of N7-protonated 1,9-DMG and 9-MG, compared with N7-protonated O^6,9-DMG. They also suggest that intersystem crossing may influence the low fluorescence quantum yields of protonated 1,9-DMG and 9-MG. The possibility that both mechanisms are important is supported by the observation that the occurrence of S_2 states, which give rise to efficient internal conversion, is often accompanied by low-lying triplet states, which permit efficient intersystem crossing.[21c] The close relationship between internal conversion within the singlet manifold and efficient intersystem crossing has been noted in earlier investigations. For example, both mechanisms have been invoked to explain the low fluorescence quantum yields of 9-carbonyl-substituted anthracenes.[21c,22c,d]

Experimental Section

Melting points were determined on a Thomas-Hoover capillary melting point apparatus and are uncorrected. Microanalyses were performed by Mr. Josef Nemeth and his staff at the University of Illinois at Urbana—Champaign. ^{1}H NMR spectra were recorded on a General Electric QE-300 spectrometer at 300 MHz. Tetramethylsilane was used as an internal standard in all NMR spectra, and the following abbreviations are used: s, singlet; d, doublet; t, triplet; m, multiplet; br, broad; and ex, exchangeable with D_2O. Ultraviolet (UV) spectra were recorded on a Beckman Acta MVI spectrophotometer. Thin-layer chromatography (TLC) was run on either Merck precoated silica gel 60 F_{254} plates or Analtech precoated silica gel plates with fluorescent indicator and the plates were visualized by irradiation with ultraviolet light.

Synthesis of 9-Methylguanine (9-MG). 2,6-Dichloropurine[27] was methylated with CH_3I/K_2CO_3 in DMSO to give a mixture of N7- and N9-methylated purine.[28] The major 2,6-dichloro-9-methylpurine was purified by crystallization from ethyl acetate and was converted to 9-methylguanine according to the procedure of Ovcharova and Golovchinskaya.[29] This was recrystallized from aqueous DMF to give analytically pure compound: mp > 300 °C; ^{1}H NMR ($(CD_3)_2SO$) δ 10.54 (s, 1 H, NH, ex), 7.63 (s, 1 H, 8-H), 6.44 (br, 2 H, NH_2, ex), 3.52 (s, 3 H, CH_3), UV, λ_{max} (pH 7) 252, 270 (sh); (pH 1) 251, 276; (pH 11) 254, 268 nm. Anal. Calcd for $C_6H_7N_5O$: C, 43.64; H, 4.27; N, 42.40. Found: C, 43.54; H, 4.27; N, 42.04.

Synthesis of 1,9-Dimethylguanine (1,9-DMG). 1-Methyl-4,5-diaminouracil[30] was converted to 1,9-dimethyl-8-thiouric acid,[31] which was converted to 1,9-dimethylguanine according to the procedure of Ovcharova et al.[32] This was recrystallized from water to give analytically pure compound: mp 277–280 °C; ^{1}H NMR ($(CD_3)_2SO$) δ 7.64 (s, 1 H, 8-H), 7.01 (s, 2 H, NH_2, ex), 3.53 (s, 3 H, CH_3), 3.31 (s, 3 H, CH_3); ^{13}C NMR ($(CD_3)_2SO$) δ 156.45, 154.08, 149.55, 138.17, 115.50, 29.02 and 27.98; UV λ_{max} (pH 7) 255, 269 (sh); (pH 1) 255, 278; (pH 11) 255, 269 (sh) nm. Anal. Calcd for $C_7H_9N_5O$: C, 46.92; H, 5.06; N, 39.08. Found: C, 46.52; H, 5.33; N, 38.78.

Synthesis of O^6,9-Dimethylguanine (O^6,9-DMG) and 1,7-Dimethylguanine. 2-Amino-6-methoxypurine[33] (660 mg, 4 mmol) and tetramethylammonium hydroxide pentahydrate (724 mg, 4 mmol) were mixed together in water (5 mL), and the solution was lyophilized. The resulting hygroscopic material was transferred to a sublimation apparatus and heated at 170–200 °C for 4 h at 0.01 mmHg pressure. The sublimed material was collected (420 mg). The ^{1}H NMR spectrum of this sublimed mixture showed the presence of at least three major compounds. The mixture was loaded on a column of silica gel packed in chloroform and eluted with a 2–20% chloroform/methanol gradient to give first O^6,9-DMG followed by 1,7-dimethylguanine, and then by 1,9-DMG in almost equal proportions. While this investigation was in progress, Kohda et al.[34] reported similar results from the alkylation of 2-amino-6-methoxypurine.

O^6,9-Dimethylguanine (O^6,9-DMG): yield 116 mg (16%); mp 194–195 °C (lit.[34] mp 194–195 °C); ^{1}H NMR ($(CD_3)_2SO$) δ 7.82 (s, 1 H, 8-H), 6.45 (s, 2 H, NH_2, ex), 3.96 (s, 3 H, OCH_3), 3.59 (s, 3 H, OCH_3), UV, λ_{max} (pH 7) 248, 279; (pH 1) 241, 288; (pH 11) 247, 279 nm. Anal. Calcd for $C_7H_9N_5O$: C, 46.92; H, 5.06; N, 39.08. Found: C, 46.62; H, 4.73; N, 39.10.

1,7-Dimethylguanine: yield 108 mg (14%); mp > 250 °C; ^{1}H NMR ($(CD_3)_2SO$) δ 7.85 (s, 1 H, 8-H), 6.67 (s, 2 H, NH_2, ex), 3.84 (s, 3 H, CH_3), 3.31 (s, 3 H, CH_3); UV, λ_{max} (pH 7) 250, 283; (pH 1) 252, 270 (sh); (pH 11) 250, 283 nm. Anal. Calcd for $C_7H_9N_5O$: C, 46.92; H, 5.06; N, 39.08. Found: C, 46.88; H, 5.14; N, 39.11.

X-ray Crystallographic Studies. Crystals for single-crystal X-ray examinations of O^6,9-DMG were grown by slow evaporation of an ethanol solution and those of 1,9-DMG were obtained from $CHCl_3$/methanol. In the crystal structure of 1,9-DMG there are four independent molecules of 1,9-DMG in the unit cell with 1.5 molecules of chloroform. The structures were solved by a direct-method SHELX-86 program.[35] Correct positions for all non-hydrogen atoms were deduced from an E map. Subsequent least-squares difference Fourier calculations in each case revealed the positions for all of the hydrogen atoms. In the case of 1,9-DMG, contributions from the chloroform hydrogen atoms were ignored. However, the remaining hydrogen atoms were included as fixed or constrained contributors in "idealized" positions. Anisotropic thermal coefficients were refined for the non-hydrogen atoms of the independent single molecules and the chlorine atoms of the fully occupied solvate molecules. Group isotropic thermal parameters were refined for the hydrogen atoms of each independent molecule and the chlorine atoms of the solvate molecule disordered about the inversion center. An isotropic thermal parameter was varied for the carbon atom of the inversion-disordered chloroform. Owing to high correlation coefficients, constraints were applied to the positional parameters of the inversion-disordered chloroform atoms and the amine hydrogen atoms; the C–Cl bond lengths were constrained to 1.76 Å and N–H bond lengths were constrained to 0.90 Å prior to each cycle of least-squares refinement. Successful refinement was indicated by maximum shift/error for the final cycles.

In the case of O^6,9-DMG, two intermolecular hydrogen bonds between H2'a and N7 [distance, 2.33 (2) Å] and H2'b and N3 [distance, 2.26 (2) Å] form infinite chains of molecules along the $b + c$ diagonal.

Photoelectron and Fluorescence Spectra. HeI photoelectron spectra were measured with a Perkin-Elmer PS 18 photoelectron spectrometer equipped with a heated probe. Temperatures at which the spectra of 1,9-DMG, O^6,9-DMG, and 9-MG were measured are 188, 184, and 201 °C, respectively. For all three compounds, successive spectra measured from a single sample over a period of 2–4 h indicated no signs of decomposition. Ionization potentials were calibrated from the $^2P_{3/2}$ and $^2P_{1/2}$ bands of Ar and Xe.

Fluorescence emission spectra were measured with a Perkin-Elmer 650-10 fluorescence spectrometer. Fluorescence lifetime measurements employed a Photochemical Research Associates Model 2000 Nanosecond fluorescence spectrometer equipped with aberration-corrected optics. Fluorescence emission experiments were carried out at 23 ± 2 °C in aqueous solution buffered with 10^{-3} M sodium cacodylate. In fluorescence measurements where the pH was varied, HCl or NaOH was added to solutions containing 1,9-DMG, O^6,9-DMG, and 9-MG. The concentrations of the methylated guanines were 5.0×10^{-5} M. Emission spectra were measured at an excitation wavelength of 270 nm. They were corrected for the wavelength dependence of the spectrometer response. This was carried out by measuring an uncorrected emission spectrum for tryptophan in distilled water and comparing it with a previously reported corrected spectrum.[36] Both the uncorrected spectrum and the reported corrected spectrum of tryptophan were obtained at an excitation wavelength of 270 nm. Fluorescence lifetime measurements were carried out at an excitation wavelength of 270 nm. The emission wavelengths were 375 nm for O^6,9-DMG and 1,9-DMG and 365 nm for 9-MG. A least-squares deconvolution method was used to analyze the lifetime data.[37]

Acknowledgment. Support of this work by the donors of the Petroleum Research Fund, administered by the American Chemical Society, the National Institutes of Health (Grant CA 41432 and GM 34125), and Cray Research Inc. is gratefully acknowledged. We wish to thank Dr. Nora Sabelli (University of Illinois at Urbana—Champaign), Drs. Willis Person and Krystyna Szczepaniak (University of Florida), and Dr. Edward

(27) Beaman, A. G.; Robins, R. K. *J. Appl. Chem.* **1962**, *12*, 432.
(28) Beaman, A. G.; Robins, R. K. *J. Org. Chem.* **1963**, *28*, 2310.
(29) Ovcharova, I. M.; Golovchinskaya, E. S. *Zh. Obshch. Khim.* **1964**, *34*, 3247.
(30) Pfleiderer, W. *Chem. Ber.* **1957**, *90*, 2272.
(31) Golovchinskaya, E. S.; Ovcharova, I. M.; Cherkasova, A. A. *Zh. Obshch. Khim.* **1960**, *30*, 3332.
(32) Ovcharova, I. M.; Nikolaeva, L. A.; Chaman, E. S.; Golovchinskaya, E. S. *Zh. Obshch. Khim.* **1962**, *32*, 2010.
(33) Balsiger, R. W.; Montgomery, J. A. *J. Org. Chem.* **1960**, *25*, 1573.
(34) Kohda, K.; Baba, K.; Kawazoe, Y. *Tetrahedron Lett.* **1987**, *28*, 6285.
(35) Sheldrick, G. M. SHELX-86. In *Crystallographic Computing 3*; Sheldrick, G. M., Kruger, C., Goddard, R., Eds.; Clarendon Press: New York, 1985; pp 175–189.
(36) Miller, J. N. *Standards in Fluorescence Spectroscopy*; Chapman and Hall: London, 1989; pp 112–113.
(37) Hui, M. H.; Ware, W. R. *J. Am. Chem. Soc.* **1976**, *98*, 4718.

Lim (University of Akron) for helpful discussions. The X-ray crystallographic data were provided by Dr. Scott R. Wilson of the University of Illinois at Urbana—Champaign. The Pittsburgh Supercomputing Center, the National Center for Supercomputing Applications at the University of Illinois at Urbana—Champaign, and the Cornell National Supercomputer Facility provided access time on CRAY X-MP/48 and IBM 3090/600 VF computers.

Registry No. 1,9-DMG, 42484-34-4; O^6,9-DMG, 61580-66-3; 9-MG, 5502-78-3.

Tautomerism and Infrared Spectra of Thiouracils. Matrix Isolation and ab Initio Studies†

H. Rostkowska,‡ K. Szczepaniak,§,⊥ M. J. Nowak,‡ J. Leszczynski,∥ K. KuBulat,§ and W. B. Person*,§

Contribution from the Institute of Physics, Polish Academy of Sciences, Al. Lotnikow 32/46, Warsaw, Poland, and the Department of Chemistry, University of Florida, Gainesville, Florida 32611. *Received July 13, 1989*

Abstract: A study of the infrared (IR) spectra of a variety of thiouracils isolated in low-temperature inert matrices demonstrated that 2- and 4-thiouracils together with their N1- and N3-methylated derivatives as well as 2,4-dithiouracil exist under these conditions only in the oxothione or dithione tautomeric forms. In contrast, S2- and S4-methylated derivatives under the same conditions exist as a mixture of hydroxy and oxo tautomeric forms. The ratio of concentrations of the tautomers K(o/h) = ([oxo]/[hydroxy]) and the free energy differences, ΔG, were experimentally estimated from the ratio of the absorbances of the NH and OH stretches. The values obtained are K(o/h) = 1.5 and ΔG = −1.7 kJ/mol for 2-(methylthio)uracil and K(o/h) = 0.5 and ΔG = +2.5 kJ/mol for 4-(methylthio)-6-methyluracil. An assignment of the observed infrared bands, particularly those related to the C=S stretching vibrations, is proposed on the basis of the comparison of the matrix spectra from different derivatives and of the spectra calculated by using ab initio methods (3-21G* basis set).

Thio derivatives of nucleosides are of interest because of their biological and pharmacological activities; e.g., as minor components of tRNA or as anticancer drugs (refs 2–8 and references therein). In particular, when 4-thiothymidine is substituted for thymidine, anomalous properties appear which are inconsistent with a Watson–Crick structure but instead agree with a left-handed double helix structure build up from Haschemeyer–Sobell (reversed Hoogsteen) base pairs.[2,5-8] Since the C_4=O group of thymidine is involved in base pairing in the Watson–Crick structure of DNA, substitution of O_4 by sulfur (in 4-thiothymidine) is expected to cause perturbation of base-pair hydrogen bonding and also of other interactions (e.g., stacking or surface interactions) of the nucleic bases.

Although thiopyrimidines identified as minor components of tRNA have been extensively studied,[9] only a few systematic investigations have been devoted to the tautomerism of thiouracils (e.g., refs 14–19 and references therein). Little attention has been given to the tautomerism of thiouracils in an inert environment,[1,15] although it is well-known that tautomeric equilibria of a number of pyrimidine bases depend strongly on intermolecular interactions of the bases (e.g., 16–21). Such inert local environments, although infrequent, might occasionally be expected to occur in the vicinity of a base or its fragment.

Even if a direct biological significance of the matrix isolation studies of biological molecules such as thiouracils might be questionable because of the "unrealistic" conditions in which molecules exist in the low-temperature inert matrix, such studies *are* necessary for testing the reliability of theoretical calculations of the properties of these molecules including their stabilities. The most reliable theoretical calculations (ab initio with good basis sets) can be performed at present only for molecules in vacuum,

Chart I

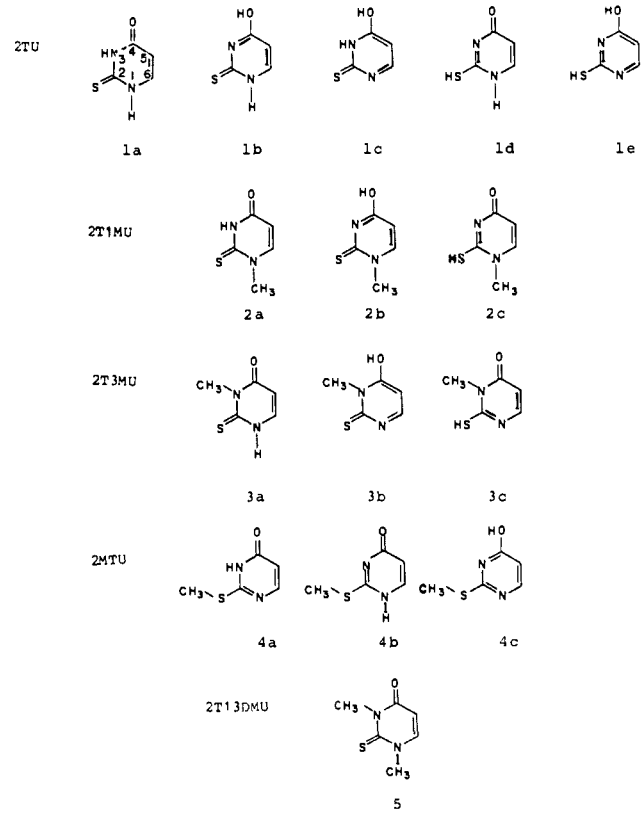

† This is Part 2 of a series of studies of thiouracils. Part 1 is ref 1.
‡ Institute of Physics, Polish Academy of Sciences.
§ Department of Chemistry, University of Florida.
⊥ At the Institute of Physics, Polish Academy of Sciences for part of this study.
∥ Department of Chemistry, University of Alabama at Birmingham.

0002-7863/90/1512-2147$02.50/0